Electric Field Modulated Nonlinear Optical Properties of Donor—Acceptor Polyenes: Sum-Over-States Investigation of the Relationship between Molecular Polarizabilities (α, β, and γ) and Bond Length Alternation

F. Meyers,[†,‡] S. R. Marder,[*,‡,§] B. M. Pierce,[⊥] and J. L. Brédas[*,†]

Contribution from the Center for Research on Molecular Electronics and Photonics, Université de Mons-Hainaut, Place de Parc 20, B-7000 Mons, Belgim, The Beckman Institute, California Institute of Technology, Pasadena, California 91125, Jet Propulsion Laboratory, California Institute of Technology, 4800 Oak Grove Drive, Pasadena, California 91109, and Hughes Aircraft Company, Radar Systems, Bldg. R02, M/S V518, P.O. Box 92426, Los Angeles, California 90009-2426

Abstract: We investigate the influence of an external, static electric field upon the relationship between the structure, spatial distribution of electron density, and linear and nonlinear polarizabilities for a set of π-electron chromophores. The bond length alternation (BLA) and the π-electron bond order alternation (BOA) in the molecular structure are calculated as a function of the external electric field strength so that the dependence of the linear polarizability, α, second-order polarizability, β, and third-order polarizability, γ, can be expressed in terms of the BLA or BOA structural parameters. The calculated effect of the external electric field on the structure and electronic properties of the chromophores is similar to that resulting from donor—acceptor substituents on a segment of the chromophore or from changing the dielectric properties of the environment around the molecule, *e.g.*, increasing the polarity of the solvent. The incorporation of a static electric field into the calculations provides a more realistic treatment of the nonlinear optical properties of the chromophore in the condensed phase and suggests strategies to optimize these properties by adjusting the dielectric properties of the medium around the chromophore.

I. Introduction

The optimization of materials for nonlinear optical (NLO) devices first requires an in-depth understanding of the NLO properties on the microscopic, or molecular, scale. Organic compounds with delocalized π-electron systems are leading candidates as NLO materials, and interest in these materials has grown tremendously in the past decade.[1-10] Reliable structure/ property relationships—where property here refers to linear polarizability, α, and first-, β, and second-, γ, hyperpolarizabilities—are required for the rational design of optimized materials for photonic devices such as electrooptic modulators and all-optical switches.

The development of organic NLO materials for device applications is a multidisciplinary effort involving both theoretical and experimental studies in the fields of chemistry, physics, and engineering. Quantum-chemical calculations have made an important contribution to the understanding of the electronic polarization underlying the molecular NLO processes and the establishment of structure—property relationships.[11,12]

The donor—acceptor substituted polymethine molecule is representative of an important class of organic NLO chromophores. Its ground-state structure can be viewed as a combination of two resonance forms, differing in the extent of charge separation, as suggested by Brooker on the basis of UV—visible spectroscopic measurements:[13]
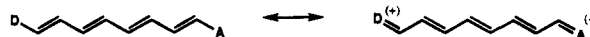
In substituted polyenes with weak donors and acceptors, the neutral resonance form dominates the ground state and the molecule has a structure with a distinct alternation in the bond-length between neighboring carbon atoms, *i.e.*, a high degree of bond length alternation (BLA). The contribution of the charge-separated resonance form to the ground state increases, and BLA decreases, when donor and acceptor substituents become stronger. The relative contribution of these two resonance forms to the ground state is also controlled by the polarity of the solvent in which the chromophore is dissolved;[14]

† Université de Mons-Hainaut.
‡ The Beckman Institute.
§ Jet Propulsion Laboratory.
⊥ Hughes Aircraft Company.
⊛ Abstract published in *Advance ACS Abstracts*, October 1, 1994.
(1) Nonlinear Optical Properties of Organics and Polymeric Materials; Williams, D. J., Ed. *ACS Symp. Ser.* **1983**, *233*.
(2) *Nonlinear Optical Properties of Organic Molecules and Crystals*; Chemla, D. S., Zyss, J., Eds.; Academic: New York, 1987.
(3) Nonlinear Optical Properties of Polymers; Heeger, A. J., Orenstein, J., Ulrich, D. R., Eds. *Mater. Res. Soc. Symp. Proc.* **1988**, *109*.
(4) Nonlinear Optical Effects in Organic Polymers; Messier, J., Kajzar, F., Prasad, P. N., Ulrich, D. R., Eds. *NATO-ARW Ser. E* **1989**, *162*.
(5) Conjugated Polymeric Materials: Opportunities in Electronics, Optoelectronics, and Molecular Electronics; Brédas, J. L., Chance, R. R., Eds. *NATO-ARW Ser. E* **1990**, *182*.
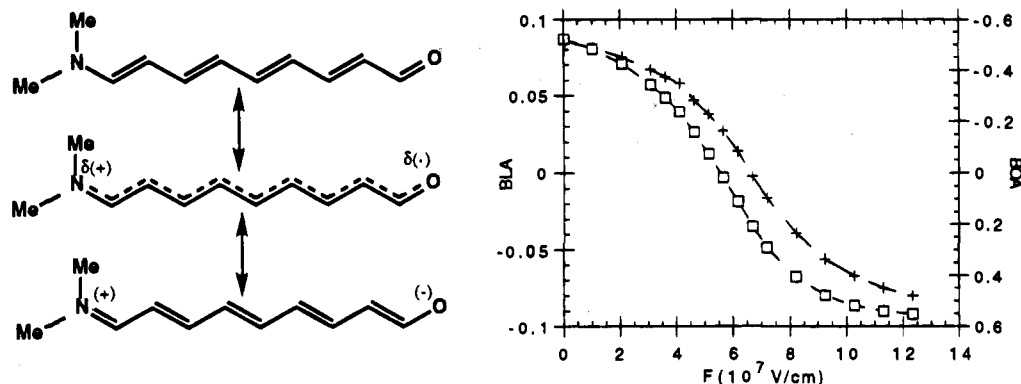(6) Prasad, P. N.; Williams, D. J. *Introduction to Nonlinear Optical Effects in Molecules and Polymers*; Wiley-Interscience: New York, 1991.
(7) Organic Molecules for Nonlinear Optics and Photonics; Messier, J., Kajzar, F., Prasad, P. N., Eds. *NATO-ARW Ser. E* **1991**, *194*.
(8) Materials for Nonlinear Optics: Chemical Perspectives; Marder, S. R., Sohn, J. E., Stucky, G. D., Eds. *ACS Symp. Ser.* **1991**, *455*.
(9) *Organic Materials for Photonics: Science and Technology*; Zerbi, G., Ed.; Elsevier Science: Amsterdam, 1993.
(10) Optical Nonlinearities in Chemistry; special issue of *Chem. Rev.* (*Jan.*) **1994**, *94*.

(11) Brédas, J. L. in ref 9, p 127.
(12) In ref 6, Section 3.5, p 42, and references therein.
(13) Brooker, L. G. S.; Sprague, R. H. *J. Am. Chem. Soc.* **1941**, *63*, 3214. Brooker, L. G. S.; Keyes, G. H.; Williams, W. W. *J. Am. Chem. Soc.* **1942**, *64*, 199. Brooker, L. G. S.; Keyes, G. H.; Sprague, R. H.; VanDyke, R. H.; VanLare, E.; VanZandt, G.; White, F. L.; Cressman, H. W. J.; Dent, J. S. G. *J. Am. Chem. Soc.* **1951**, *73*, 5326. Brooker, L. G. S.; Craig, A. C.; Heseltine, D. W.; Jenkins, P. W.; Lincoln, L. L. *J. Am. Chem. Soc.* **1965**, *87*, 2443.

Figure 1. (Left) Canonical resonance structures for the 9-(dimethylamino)nona-2,4,6,8-tetraenal molecule, DAO: (top) neutral polyene limit; (middle) cyanine limit; (bottom) zwitterionic charge-separated limit. (Right) Corresponding evolution of bond length alternation, BLA (in Å, crosses), and bond order alternation, BOA (squares), as a function of the applied external electric field F.

Figure 2. Canonical resonance structures for the cyanine molecule investigated in this work: bis(dimethylamino)nonamethine.

a more polar solvent increases the ground-state polarization, which makes the charge-separated form more dominant. Experiments have clearly demonstrated that the medium influences to a large extent the molecular geometry,[14-16] and as a direct consequence, the NLO properties.[17-19] This effect of the solvent medium on the NLO properties is consistent with the linear optical solvatochromic response well documented for many organic dyes.[20] As a result, calculations on isolated molecules (*i.e.*, in the "gas phase") are helpful, but far from being able to reproduce accurately experimental data, such as the results of solvent-dependent hyperpolarizability measurements.[17,18] Consequently, an important new step in the calculation of NLO properties would be to take explicitly into account the influence of the medium surrounding the NLO chromophore. Most treatments[21-23] of the dielectric medium are based on the reaction model of Onsager, well described in the book by Böttcher;[24] recently this model has been applied by a number of authors[25] to study the influence of solvent on the NLO response of organic molecules, at both the semiempirical and ab initio levels.

In this work, we take the first step beyond "gas-phase" calculations by examining the influence of an external static electric field on chromophores such as linear polymethine dyes. This external static electric field has been found to be efficient in controlling the ground-state polarization of the chromophores investigated in this work and, therefore, useful in simulating the qualitative effect of the solvent medium on nuclear geometry, electronic structure, and optical properties.[26] The major advantage of our approach, relative to reaction field theory, is that it allows us to follow the evolution of the molecular properties from the polyene neutral form to the fully charge-separated form and therefore to get a more complete picture.

The theoretical methodology is outlined in Section II. In Sections III–V, we present and discuss our calculations for the 9-(dimethylamino)nona-2,4,6,8-tetraenal molecule; this compound thus corresponds to an octatetraene segment end-capped by dimethylamino and aldehyde groups and is denoted DAO (Figure 1). The results of geometry optimizations for DAO as a function of external electric field strength and the evolution of the charge distribution are described in Section III. Section IV is devoted to a discussion of the electronic structure with respect to the strength of the electric field applied along the main axis of the chromophore. The electric field dependence of the static polarizabilities α, β, and γ is presented and discussed in Section V. In order to verify that the structure/ properties relationships that result from the analysis of DAO can be applied to a wider range of polymethine dyes, we also investigated a symmetric cyanine cation related to DAO, bis-(dimethylamino)nonamethine: $[(CH_3)_2-N-(CH=CH)_4-CH=N-(CH_3)_2]^+$ (Figure 2). In Section VI, the electronic structure and NLO properties of this cyanine are presented in comparison to those of DAO. In Section VII, we compare the electric field dependence of α, β, and γ for four donor–acceptor chromophores including DAO, which are distinguished by different substituents at each end of the octatetraene moiety. Finally, in Section VIII, we study the dynamic, or frequency-dependent, polarizability tensor components for the main axis (X-axis) of DAO: $\alpha_{XX}(\omega;\omega)$, $\beta_{XXX}(-2\omega;\omega,\omega)$ for second harmonic generation, and $\gamma_{XXXX}(-3';\omega,\omega,\omega)$ for third harmonic generation.

(14) Marder, S. R.; Perry, J. W.; Tiemann, B. G.; Gorman, C. B.; Gilmour, S.; Biddle, S. L.; Bourhill, G. *J. Am. Chem. Soc.* **1993**, *115*, 2524.

(15) Benson, H. G.; Murell, J. N. *J. Chem. Soc., Faraday Trans. 2* **1972**, *68*, 137.

(16) Radeglia, R.; Dähne, S. *J. Mol. Struct.* **1970**, *5*, 399. Radeglia, R.; Engelhardt, G.; Lippmaa, E.; Pehk, T.; Nolte, K. D.; Dähne, S. *Org. Magn. Reson.* **1972**, *4*, 571. Radeglia, R.; Steiger, T. *J. Prakt. Chem.* **1991**, *333*, 505.

(17) Bourhill, G.; Brédas, J. L.; Cheng, L. T.; Marder, S. R.; Meyers, F.; Perry, J. W.; Tiemann, B. G. *J. Am. Chem. Soc.* **1994**, *116*, 2619.

(18) Marder, S. R.; Perry, J. W.; Bourhill, G.; Gorman, C. B.; Tiemann, B. G.; Mansour, K. *Science* **1993**, *261*, 186.

(19) Clays, K.; Hendrichkx, E.; Triest, M.; Verblest, T.; Persoons, A.; Dehu, C.; Brédas, J. L. *Science* **1993**, *262*, 1419.

(20) Reichardt, C. *Solvents and Solvent Effects in Organic Chemistry*; VCH: Weinheim, 1988.

(21) Rivail, J. L.; Rinaldi, D. *Chem. Phys.* **1976**, *18*, 233. Rinaldi, D.; Ruiz-Lopez, M. F.; Martins Costa, M. T. C.; Rivail, J. L. *Chem. Phys. Lett.* **1986**, *128*, 177.

(22) Wah Wong, M.; Frisch, M. J.; Wilberg, K. B. *J. Am. Chem. Soc.* **1991**, *113*, 4776. Wah Wong, M.; Wilberg, K. B.; Frisch, M. J. *J. Chem. Phys.* **1991**, *95*, 8991.

(23) Karelson, M. M.; Zerner, M. C. *J. Phys. Chem.* **1992**, *96*, 6949.

(24) Onsager, L. *J. Am. Chem. Soc.* **1936**, *58*, 1486. Böttcher, C. J. F. *Theory of Electric Polarization: Dielectrics in Static Fields*; Elsevier: Amsterdam, 1973.

(25) Willetts, A.; Rice, J. E. *J. Chem. Phys.* **1993**, *99*, 426. Mikkelsen, K. V.; Luo, Y.; Agren, H.; Jorgensen, P. *J. Chem. Phys.* **1994**, *100*, 8240. Yu, J.; Zerner, M. C. *J. Chem. Phys.* **1994**, *100*, 7487. Di Bella, S.; Marks, T. J.; Ratner, M. A. *J. Am. Chem. Soc.* **1994**, *116*, 4440.

(26) Nolte, K. D.; Dähne, S. *Adv. Mol. Relax. Inter. Proc.* **1977**, *10*, 299.

II. Methodology

All the molecular orbital calculations reported here were performed using the semiempirical Intermediate Neglect of Differential Overlap (INDO)[27,28] Hamiltonian, and proceed in three steps: (i) optimization of the molecular structure under the influence of an external homogeneous static electric field applied along the long axis of the molecule and directed in such a way as to favor charge transfer from the donor to the acceptor; (ii) calculation of the transition energies, state dipole moments, and transition dipole moments, using the configuration interaction (CI) technique[28] [the CI employed here includes single (S) excitations between all π-molecular orbitals (MO's) and double (D) excitations among the four highest occupied π-MO's and four lowest unoccupied π^*-MO's (SDCI-calculation)]; and (iii) evaluation of the Sum-Over-States (SOS)[29] expression for the polarizability α and hyperpolarizabilities β and γ [the summation is performed over 30 states, which we have checked is sufficient to obtain converged values of the molecular polarizabilities in the case of the compounds investigated here].

The SOS expressions for the dominant components of the static first-, second-, and third-order polarizability tensors are (within a Taylor series expansion):

$$\alpha_{XX} = 2 \sum_{m \neq g} \frac{\langle g|\mu_X|m\rangle\langle m|\mu_X|g\rangle}{E_{gm}} \tag{1}$$

$$\beta_{XXX} = 6 \sum_{m \neq g} \sum_{n \neq g} \frac{\langle g|\mu_X|m\rangle\langle m|\bar{\mu}_X|n\rangle\langle n|\mu_X|g\rangle}{E_{gm}E_{gn}} \tag{2}$$

$$\gamma_{XXXX} = 24 \left(\sum_{m \neq g} \sum_{n \neq g} \sum_{p \neq g} \frac{\langle g|\mu_X|m\rangle\langle m|\bar{\mu}_X|n\rangle\langle n|\bar{\mu}_X|p\rangle\langle p|\mu_X|g\rangle}{E_{gm}E_{gn}E_{gp}} - \sum_{m \neq g} \sum_{p \neq g} \frac{\langle g|\mu_X|m\rangle\langle m|\mu_X|g\rangle\langle g|\mu_X|p\rangle\langle p|\mu_X|g\rangle}{E_{gm}E_{gp}E_{gp}} \right) \tag{3}$$

Here X corresponds to the long axis of the molecules; $\langle g|\mu_X|m\rangle$ is the electronic transition moment along the Cartesian X-axis between the reference state $\langle g|$ (i.e., here the ground state) and excited state $\langle m|$; $\langle m|\bar{\mu}_X|n\rangle$ denotes the dipole difference operator equal to $\langle m|\mu_X|n\rangle - \langle g|\mu_X|g\rangle\delta_{mn}$, where δ_{mn} is the Kronecker delta function; E_{gm} is the energy difference between states $|m\rangle$ and $|g\rangle$.

These expressions become slightly modified when the dynamic NLO properties are evaluated. To calculate the first-order process $\alpha_{XX}(-\omega;\omega)$, the denominator in eq 1 becomes:

$$E_{gm} - \bar{h}\omega - i\Gamma_{gm}$$

The $\beta_{XXX}(-2\omega;\omega,\omega)$ second-harmonic-generation term is evaluated by changing the denominator in eq 2 to:

$$(E_{gm} - 2\bar{h}\omega - i\Gamma_{gm})(E_{gn} - \bar{h}\omega - i\Gamma_{gn})$$

while in the calculation of the $\gamma_{XXXX}(-3\omega;\omega,\omega,\omega)$ third-harmonic-generation term, the denominators in eq 3 become:

$$(E_{gm} - 3\bar{h}\omega - i\Gamma_{gm})(E_{gn} - 2\bar{h}\omega - i\Gamma_{gn})(E_{gp} - \bar{h}\omega - i\Gamma_{gp})$$

and

$$(E_{gm} - 3\bar{h}\omega - i\Gamma_{gm})(E_{gp} - \bar{h}\omega - i\Gamma_{gp})(E_{gp} + \bar{h}\omega - i\Gamma_{gp})$$

In these expressions ω is the frequency of the perturbating radiation field and Γ_{gm} is the damping factor associated with excited state $|m\rangle$.

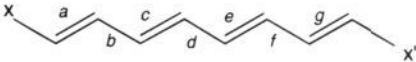## III. Geometry Optimization and Charge Distributions

The optimized structures of the octatetraene and DAO molecules, calculated using the INDO Hamiltonian, are reported

(27) Pople, J. A.; Beveridge, D. L.; Dobosh, P. A. *J. Chem. Phys.* **1967**, *47*, 2026.

(28) Ridley, J.; Zerner, M. C. *Theor. Chim. Acta* **1973**, *32*, 111.

(29) Orr, B. J.; Ward, J. F. *Mol. Phys.* **1971**, *20*, 513.

Table 1. INDO-Optimized Bond Lengths (Å) in Octatetraene (X = X′ = H) and DAO (X = NMe₂ and X′ = CHO); the Geometric Structure Evolution of DAO under the Influence of a Static External Electric Field F (in 10^7 V/cm) Is Also Reported


|		bond lengths, Å							
F	X	a	b	c	d	e	f	g	X′
0	H	1.336	1.448	1.349	1.445	1.349	1.448	1.336	H
0	NMe₂	1.356	1.438	1.354	1.440	1.353	1.440	1.352	CHO
2	NMe₂	1.361	1.432	1.359	1.434	1.358	1.435	1.356	CHO
5	NMe₂	1.380	1.411	1.378	1.414	1.375	1.418	1.371	CHO
10	NMe₂	1.428	1.360	1.432	1.361	1.431	1.366	1.422	CHO

in Table 1. The results first show that the substituents act to reduce the length of the single bonds and to increase the length of the double bonds, *in the absence of any external field*. As a consequence, the bond length alternation (BLA) decreases from 0.102 Å to 0.086 Å when the dimethylamino and aldehyde functionalities substitute at opposite ends of the polyene chain. The BLA is defined here as the average of the difference in length between adjacent single and double bonds (it is by convention taken to be positive in the neutral canonical resonance form).

The calculated decrease in BLA for the substituted polyene can be explained as originating from an *internal* electric field, F_i, imposed on the octatetraene segment due to the presence of the donor/acceptor end groups. An estimate of F_i can be obtained by determining the strength of the electric field that needs to be applied to the unsubstituted octatetraene molecule in order to reproduce the same BLA as in the center of the DAO molecule. The magnitude of this internal field F_i induced by the dimethylamino and aldehyde functionalities is calculated to be on the order of 7×10^7 V/cm. The magnitude of F_i associated with other donor and acceptor substituents is reported in Section VI.

In Table 1, we also follow the change in geometry for DAO when a static external electric field, F, is applied along the long axis of the molecule. A field strength of about 2×10^7 V/cm (in the direction that favors charge transfer from the donor end to the acceptor end) is required for the geometry to start evolving in such a way that the single bonds become significantly shorter and the double bonds longer, compared to the situation where no field is applied. Increasing the strength of F induces a continuous decrease in BLA, which eventually becomes equal to zero. A zero-BLA situation is usually observed in a cyanine-type molecule (Figure 2); the ground-state structure of a cyanine in the absence of an external electric field is described by an
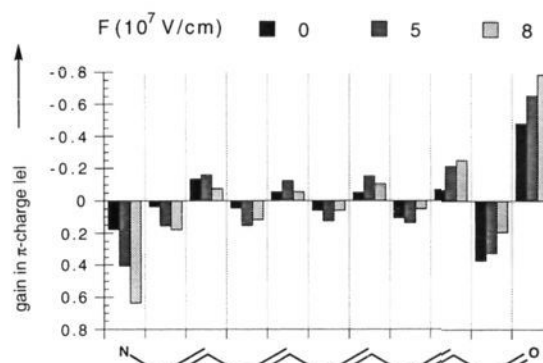
Figure 3. Histogram of the INDO/SDCI atomic π-charges (in |e|) in the ground state of DAO, when $F = 0$, 5×10^7, and 8×10^7 V/cm.
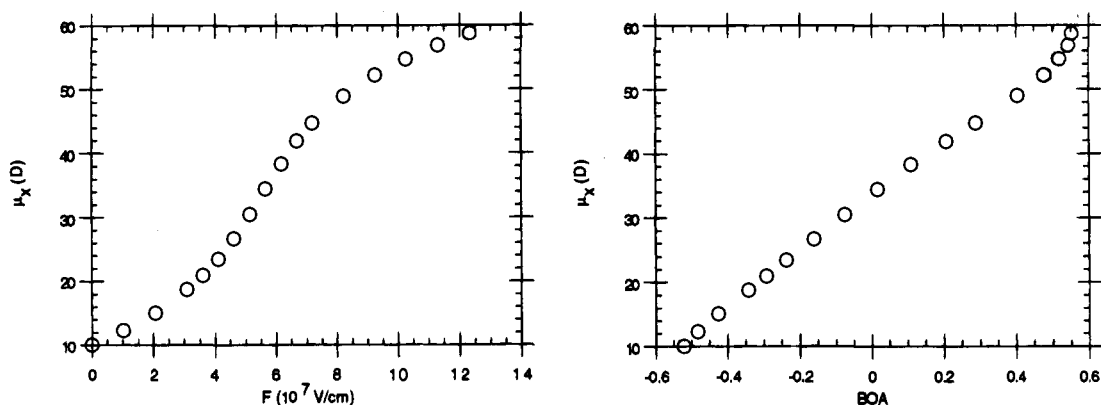
Figure 4. Evolution in DAO of the INDO/SDCI X-component of the dipole moment, μ_X (in Debye), as a function of the applied electric field strength F (left) and plotted versus BOA (right).

equal contribution of each resonance form, which results in a zero BLA. For this reason, in this paper, a zero-BLA situation is referred to as the cyanine limit. In the case of the donor/acceptor pair in the DAO molecule, the cyanine limit is achieved for an electric field of approximately 6.5×10^7 V/cm. An alternation in the single/double bond pattern resumes at higher field strengths. However, this alternation is reversed with respect to the situation in the neutral polyene limit, and the ground-state structure becomes increasingly dominated by the zwitterionic resonance form. Complete BLA reversal occurs at a field of about 10^8 V/cm. The evolution of BLA as a function of the applied electric field F is displayed in Figure 1.

It is important to stress that this range in electric field strength from $\approx 10^7$ to 10^8 V/cm is on the same order as the reaction fields determined for common dipolar liquids; for instance, the reaction field in chloroform is 0.9×10^7 V/cm, and that in acetonitrile is 6.8×10^7 V/cm.[25] It thus appears that the external electric field strengths employed in our approach are similar to what a dipolar molecule may experience upon going from the gas phase to condensed phases, such as polar solvents.[20]

The difference in π-bond orders between adjacent bonds defines a bond-*order* alternation (BOA), which is directly related to BLA in conjugated π-electron compounds.[30] The small differences between BLA and BOA seen in Figure 1 are only due to our methodology. More specifically, the electric field required to reach the cyanine limit defined by BLA is about 6.5×10^7 V/cm whereas this field is slightly smaller (≈ 5 to 5.5×10^7 V/cm) when defined by BOA. This can be explained by the fact that the INDO calculations are using two different sets of parameters for the electron repulsion integrals: (i) one set is taken for geometry optimizations,[28] from which BLA is evaluated; and (ii) a second set, based on the Ohno–Klopman integral,[31] is used in the SDCI calculations,[32-35] from which we derive the BOA values.

In Figure 3, the INDO/SDCI atomic π-charge distributions in the ground state of DAO are plotted in histogram form for three electric field strengths: when $F = 0$ (*i.e.*, the polyene limit), $F = 5 \times 10^7$ V/cm (*i.e.*, the cyanine limit), and $F = 8 \times 10^7$ V/cm. It is clearly observed that the interaction between the field and the molecule induces a shift in electron density from the dimethylamino donor group toward the aldehyde

acceptor end. When the field increases from 0 to 5×10^7 V/cm, the amount of π-charge is reduced at the donor end by about $0.2|e|$ (going from $+0.18|e|$ to $+0.41|e|$ on the nitrogen of the donor end) and simultaneously enhanced at the acceptor end. We also note that a net π-charge alternation pattern (charge density wave) is induced upon the carbon atoms in the middle of the molecule; from $F = 0$ to 5×10^7 V/cm, the difference in π-electron charge between adjacent carbons roughly triples, going from about $0.1|e|$ to $0.3|e|$, which results in a strong polarization of the carbon–carbon bonds. When the field goes from 5 to 8×10^7 V/cm, the amount of π-charge is reduced further at the donor end and enhanced at the acceptor end. As a consequence, the ground-state dipole moment keeps increasing upon application of stronger electric fields. On the other hand, it is interesting to note that the π-charge alternation actually reaches a maximum when the field is about 5×10^7 V/cm, *i.e.*, the cyanine limit: by increasing the field from 5 to 8×10^7 V/cm, the alternation in π-electron charge between adjacent carbons decreases and is about $0.15|e|$ when $F = 8 \times 10^7$ V/cm. The evolution of the X-component of the dipole moment, μ_X, as a function of F is illustrated in the left part of Figure 4. We observe that it has the same shape as the evolution of BLA or BOA as a function of F and consequently, plotted versus BOA, μ_X presents a more linear function (Figure 4, right).

IV. Electronic Structure

In π-conjugated organic systems, the molecular geometry and the electronic structure are strongly related.[30,36] This feature and its chemical and physical consequences have been addressed extensively in the field of conducting polymers for over a decate[37,38] but also more recently in organic nonlinear optics.[18,19,39] It is therefore of interest to investigate the energy evolution of the π-MO's (at the Hartree–Fock level) as a function of F, and therefore as a function of BOA evolution.

The application of an electric field from $F = 0$ to 5×10^7 V/cm leads to a destabilization of the Highest Occupied Molecular Orbital (HOMO) (Figure 5). In order to understand the origin of this destabilization, it is informative to analyze the evolution as a function of F, of the bonding–antibonding pattern in the corresponding orbital wavefunction. The HOMO starts being destabilized because electronic characteristics pertaining to the (unperturbed) Lowest Unoccupied Molecular Orbital (LUMO) are being introduced at the acceptor end, see

(30) Salem, L. *The Molecular Orbital Theory of Conjugated Systems*; W. A. Benjamin: New York, 1966.

(31) Ohno, K. *Theor. Chim. Acta* **1964**, *2*, 219.

(32) Shulten, K.; Ohmine, I.; Karplus, M. *J. Chem. Phys.* **1976**, *64*, 4422.

(33) Ducasse, L. R.; Miller, T. E.; Soos, Z. G. *J. Chem. Phys.* **1982**, *76*, 4094.

(34) Tavan, P.; Schulten, K. *J. Chem. Phys.* **1986**, *85*, 6602. Tavan, P.; Schulten, K. *Phys. Rev. B* **1987**, *36*, 4337.
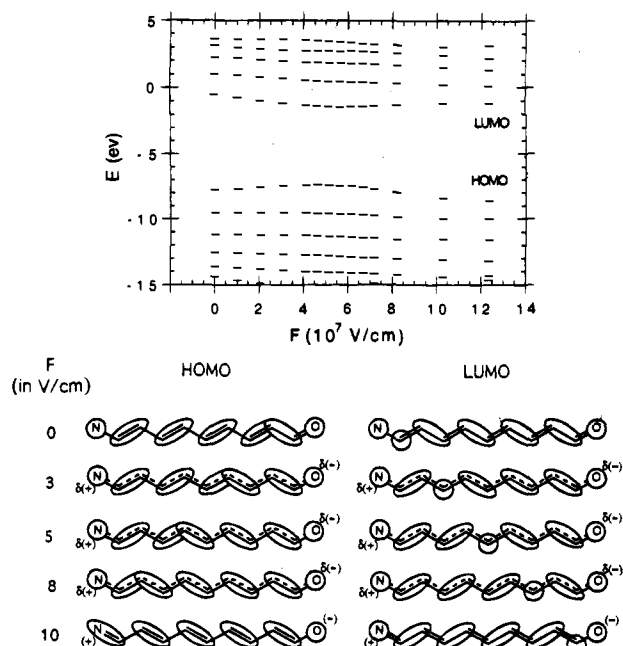
(35) Pierce, B. M. *J. Chem. Phys.* **1989**, *91*, 791.

(36) Brédas, J. L. *Science* **1994**, *263*, 487.

(37) Brédas, J. L.; Street, G. B. *Acc. Chem. Res.* **1985**, *18*, 309.

(38) Heeger, A. J.; Kilvelson, S.; Schrieffer, J. R.; Su, W. P. *Rev. Mod. Phys.* **1988**, *60*, 782.

(39) Gorman, C. B.; Marder, S. R. *Proc. Natl. Acad. Sci. U.S.A.* **1993**, *90*, 11297.
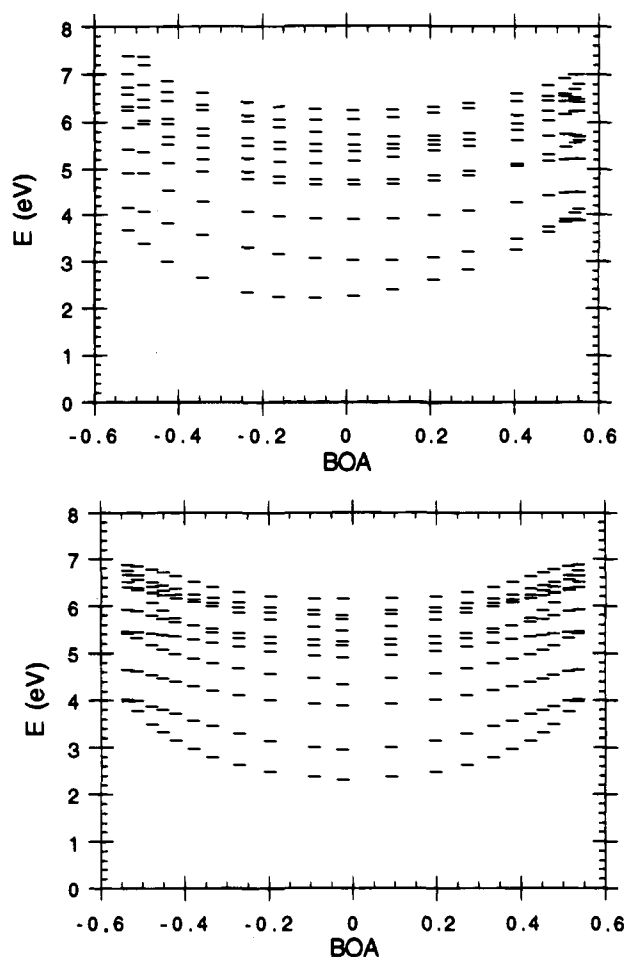
Optical Properties of Donor–Acceptor Polyenes

J. Am. Chem. Soc., Vol. 116, No. 23, 1994   10707

Figure 5. (Top) Evolution of the INDO highest occupied π-MO's and lowest unoccupied π^*-MO's as a function of F. (Bottom) Sketch of the nodal patterns in the HOMO and LUMO wave functions of DAO superimposed upon the ground-state geometric structure, when the applied electric field F (in 10^7 V/cm) is 0, 3, 5, 8, and 10.

Figure 5. Under the influence of an intermediate strength field (Figure 5, for $F = 3$ to 8×10^7 V/cm), the bonding–antibonding pattern for the HOMO is fully reversed at the acceptor end as well as in the adjacent part of the polyene segment. For fields beyond 5×10^7 V/cm, the HOMO level gets stabilized; this is due to the fact that, under the influence of the electric field, the geometric structure is simultaneously modified and eventually makes the reversal process in bonding–antibonding characters of the HOMO wave function energetically favorable. Globally, for the LUMO level, a stabilization, followed by a destabilization, is observed and can be understood in a fully similar way.

We now turn to a discussion of the evolution of the $^1\pi\pi^*$ excited-state energies as a function of electric field F. At this stage, it is useful to point out that, because of the presence of the donor and acceptor groups, the symmetry of the DAO molecule is low and belongs to the C_s point group. As a result, and unlike the situation in centrosymmetric polyenes, all transitions between singlet π-states are allowed. We also note that the lowest excited singlet state in DAO, S_1, is very similar to the ^1B_u $^1\pi\pi^*$ excited state of the octatetraene molecule. Both the S_1 state in DAO and the ^1B_u state in octatetraene are largely defined by a HOMO $\rightarrow$ LUMO single excitation, and both have a very large one-photon oscillator strength. The major difference between the two molecules is that the ^1B_u state in octatetraene is the second excited singlet state, S_2.[40]

As qualitatively expected from the dependence of the HOMO and LUMO levels on the external electric field shown in Figure 5, when the field increases from 0 (polyene limit; BOA $\approx$ −0.5) to 5×10^7 V/cm (cyanine limit; BOA $\approx$ 0), we calculate a decrease in the first transition energy (Figure 6). That corresponds to a situation where, through the interaction with the electric field, the first excited state S_1 is preferentially stabilized with respect to the ground state S_0 (bathochromic shift). This can be easily explained by the fact that the S_1 state dipole moment is larger than that in the ground state; the dipole

(40) Kohler, B. In *Conjugated Polymers: The Novel Science and Technology of Highly Conducting and Nonlinear Optically Active Materials*; Brédas, J. L., Silbey, R., Eds.; Kluwer: Dordrecht, 1991; p 405.

Figure 6. Evolution of the INDO/SDCI lowest excited-state energies in the 9-(dimethylamino)nona-2,4,6,8-tetraenal molecule, DAO (top), and bis(dimethylamino)nonamethine (bottom) as a function of BOA.

moment thus increases during the electronic transition. This red shift in the $S_0 \rightarrow S_1$ transition takes place up to the point where the ground state becomes described by equal contributions from the polyene form and the charge separated form, *i.e.*, in the cyanine limit. Beyond this point, under the influence of electric fields $F > 5 \times 10^7$ V/cm (BOA > 0), a blue shift is observed; the ground state is then more stabilized than the first excited state through the interaction with the electric field, the dipole moment decreasing during the electronic transition. This electrochromic behavior is consistent with the closely related solvatochromic behavior observed for numerous merocyanine molecules.[13,15,20,26]

V. Molecular Polarizabilities

The correlated ground- and excited-state dipole moments and transition dipole moments are calculated for the optimized molecular geometry using the INDO/SDCI procedure. We can then compute the linear polarizability α and hyperpolarizabilities β and γ, using the SOS formulation. Since the molecule has a linear shape, the polarizabilities were found to be totally dominated by the longitudinal tensor components (here along the X-axis). The evolution of the α_{xx}, β_{xxx}, and γ_{xxxx} components is plotted versus BOA (and thus as function of F) in Figure 7.

a. The Linear Polarizability α. We observe that, plotted versus BOA, the linear polarizability α_{xx} follows a simple evolution: it peaks at the cyanine limit (BOA $\approx$ 0), with the minimum values associated with the neutral polyene and charge-separated forms, in agreement with previous predictions[39,41] and

10708 *J. Am. Chem. Soc., Vol. 116, No. 23, 1994*

Meyers et al.
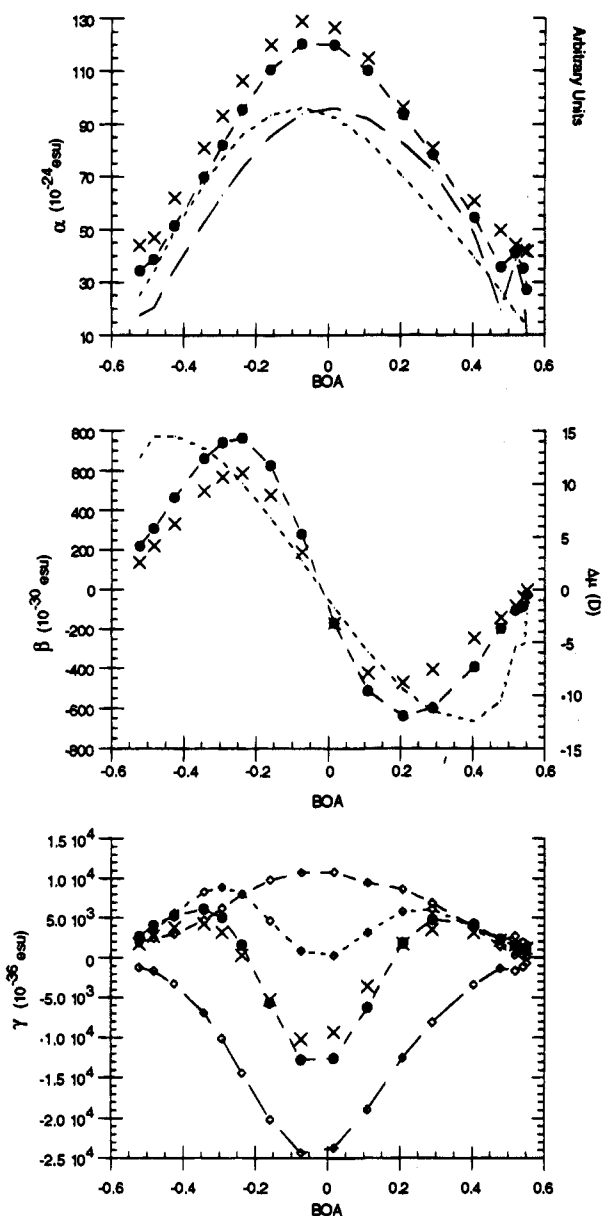
Figure 7. Evolutions in DAO plotted vs BOA of (top) α_{XX}[SOS] (crosses) and α_{XX}[model] (full circles, dashed line), in 10^{-24} esu [the inverse of E_{ge} (short dashed line) and the transition dipole moment M_{ge} (long dashed line) in arbitrary units], (middle) β_{XXX}[SOS] (crosses) and β_{XXX}[model] (full circles, dashed line) in 10^{-30} esu [$\Delta\mu$ (short dashed line) in Debye], and (bottom) γ_{XXXX}[SOS] (crosses) and γ_{XXXX}[model] (full circles, dashed line), and the D- (diamonds, short dash line), N- (diamonds, long dashed line) and T-terms (diamonds, medium dashed line), all in 10^{-36} esu.

experimental observation.[42] It is of interest to compare the fully converged SOS values, α_{XX}[SOS], to the results obtained with a simplified formula in which only a single excited state with a high one-photon absorptivity (usually S_1) is considered (*i.e.*, a two-state (S_0 and S_1) model). In this case, the SOS expression for α_{XX} (eq 1) simplifies to:

$$\alpha_{XX[model]} = 2\frac{\langle g|\mu_X|e\rangle\langle e|\mu_X|g\rangle}{E_{ge}} = 2\frac{M_{ge}^2}{E_{ge}} \quad (4)$$

where $|g\rangle = S_0$ and $|e\rangle = S_1$; the linear polarizability in this

(41) Bodart, V. P.; Delhalle, J.; André, J. M.; Zyss, J. *Can. J. Chem.* **1985**, *63*, 1631. André, J. M.; Barbier, C.; Bodart, V. P.; Delhalle, J. in ref 2, Vol. II, p 137.

(42) Dähne, S.; Nolte, K. D. *J. Chem. Soc., Chem. Comm.* **1972**, 1056.

model, α_{XX}[model], is thus simply proportional to the square of the transition dipole moment between the ground state and the first excited state, M_{ge}, and inversely proportional to the first transition energy, E_{ge}.

The electric field dependence of M_{ge} and $1/E_{ge}$ is reported in the top of Figure 7, where they are plotted versus BOA. The shape and magnitude of the curve for linear polarizability vs BOA are well reproduced by the simple model. The "two-state model" thus constitutes a good approximation to describe the F dependence of the linear polarizability in such donor—acceptor polyenes. Through this model, the evolution of α can be easily understood. The first transition energy evolves with the applied electric field in such a way that, as a function of BOA, $1/E_{ge}$ peaks at the cyanine limit (Figure 7, top). Furthermore, the transition dipole moment M_{ge} between the ground state and S_1 evolves in a similar way as a function of BOA. These behaviors have been depicted both theoretically[15,26,43] and experimentally.[13] The product $1/E_{ge}$ times M_{ge}^2, which constitutes α_{XX}[model], then evolves, as a function of BOA, in such a way as to be maximized at the cyanine limit, where BOA = 0.

One should note that similar results, showing that in polyenes α increases with decreasing bond alternation, have also been described, *e.g.*, by Bodart *et al.*[41] or deMelo and Silbey[44] (in the latter case, a decrease in BOA was forced by the formation of soliton defects).

b. The First Hyperpolarizability β. The electric field dependence of the first hyperpolarizability β is more complex than that of α: β first increases with increasing magnitude of the field, peaks in a positive sense, decreases, passes through zero, becomes negative, peaks in a negative sense, and finally increases again to become small for the charge-separated form of the DAO molecule (Figure 7, middle).

We can also compare the SOS results, β_{XXX}[SOS], to those of the traditional two-state model proposed by Oudar and Chemla,[45] β_{XXX}[model], in which only the ground state $|g\rangle$ and the first excited state $|e\rangle$ are considered. In this case, the SOS expression for β_{XXX} (eq 2) simplifies to:

$$\beta_{XXX[model]} = 6\frac{\langle g|\mu_X|e\rangle(\langle e|\mu_X|e\rangle - \langle g|\mu_X|g\rangle)\langle e|\mu_X|g\rangle}{E_{ge}^2} \quad (5)$$

$$= 6\frac{M_{ge}^2\Delta\mu}{E_{ge}^2} \quad (6)$$

where $\Delta\mu$ is then the difference between the dipole moments in the first excited state and the ground state. As has been discussed by Marder and co-workers,[43,46] the shape for β versus BOA results from a compromise between $\Delta\mu$ on one hand and $1/E_{ge}^2$ and M_{ge}^2 on the other hand. This model has provided design guidelines for optimization of β that have resulted in molecules with significantly improved properties.[47]

The evolution of β_{XXX}[model] as a function of BOA is similar to that of β_{XXX}[SOS] (Figure 7, middle); the model also reproduces the magnitude of β with an accuracy of $\approx 80\%$. As noted before,

(43) Marder, S. R.; Beratan, D. N.; Cheng, L. T. *Science* **1991**, *252*, 103.

(44) deMelo, C. P.; Silbey, R. *J. Chem. Phys.* **1988**, *88*, 2558.

(45) Oudar, J. L.; Chemla, D. S. *J. Chem. Phys.* **1977**, *66*, 2664. Oudar, J. L. *J. Chem. Phys.* **1977**, *67*, 446.

(46) Risser, S. M.; Beratan, D. N.; Marder, S. R. *J. Am. Chem. Soc.* **1993**, *115*, 7719.

(47) Marder, S. R.; Cheng, L. T.; Tiemann, B. G.; Friedly, A. C.; Blanchard-Desce, M.; Perry, J. W.; Skindhoj, J. *Science* **1994**, *263*, 511.
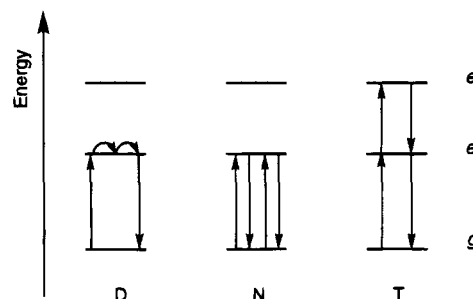
the $1/E_{ge}$ (and therefore $1/E_{ge}^2$) and M_{ge}^2 terms peak at the cyanine limit. The evolution of the $\Delta\mu$ term is very different and is the origin of the more complex evolution of β vs α. Starting from the polyene limit, $\Delta\mu$ first increases and reaches a maximum around BOA = −0.45; thereafter, it decreases and passes through zero at roughly the cyanine limit (this means that, at this point, S_0 and S_1 possess identical dipole moments, which both correspond to a partial charge transfer from the donor to the acceptor); $\Delta\mu$ then becomes increasingly negative and reaches a minimum around BOA = +0.40; after that, it increases again and tends toward a small negative value in the zwitterionic limit (Figure 7, middle). The small $\Delta\mu$ in that limit is a consequence of large but nearly equal dipole moments in both the S_1 and S_0 states. These features in the evolution of $\Delta\mu$ have already been discussed in 1977 by Dähne and Nolte[42] and reexamined in the context of the first-order hyperpolarizability by Marder and co-workers.[39,43]

Overall, we thus observe that the evolution of $\beta_{XXX[\text{model}]}$ as a function of BOA is very similar to that of $\Delta\mu$, except that the two extrema for β are pushed closer to the cyanine limit due to the influence of the M_{ge}^2/E_{ge}^2 term peaking at that limit (the positive and negative peaks for β occur at BOA values equal to −0.25 and +0.20, respectively).

The experimental demonstration of the dependence in β in donor/acceptor substituted polyenes on the ground-state polarization and consequently the bond alternation has been reported recently.[17] In these experiments, solvents of increasing polarity and substituents of increasing strength are used to control the molecular structure of the chromophores; simultaneously, the $\mu\beta$ values are obtained from EFISHG measurements. These results indicate that the various regions in the β curve evolution can be mapped out by using different donor/acceptor polyenes. This allows for a fine control in the design of new chromophores for second-order NLO properties.

c. The Second-Order Hyperpolarizability γ.

The evolution of the second-order hyperpolarizability γ as a function of the external field F gets more complex than those of α and β. The γ curve has two positive peaks associated with two intermediate forms that appear (i) between the neutral-polyene and cyanine-like structures and (ii) between the cyanine-like and totally charge-separated forms. At the cyanine limit, γ has a large negative peak. A negative value of γ physically corresponds to a situation where the molecular polarization decreases with increasing laser intensity. This negative non-linear refractive index leads to the self-defocussing of an intense beam of light.

Here also, we compare the results of the SOS calculations, $\gamma_{XXXX[\text{SOS}]}$, to those of a simplified model $\gamma_{XXXX[\text{model}]}$.[48–51] The model expression for γ is obtained from the SOS expression (eq 3) by considering that, as in the cases described above for α and β, the ground state $|g\rangle$ is strongly coupled to a single excited state $|e\rangle$ ($|m\rangle$ and $|p\rangle$ in eq 3) and that this excited state $|e\rangle$ is itself strongly coupled to only a few other excited states

(48) Kuzyk, M. G.; Dirk, C. W. *Phys. Rev. A* **1990**, *41*, 5098. Dirk, C. W.; Cheng, L. T.; Kuzyk, M. G. *Int. J. Quantum Chem.* **1992**, *43*, 27.
(49) Garito, A. F.; Heflin, J. R.; Wong, K. Y.; Zamani-Khamiri, O. *Proc. SPIE-Int. Soc. Opt. Eng.* **1988**, *971*, 2. Garito, A. F.; Heflin, J. R.; Wong, K. Y.; Zamani-Khamiri, O. In Organic Materials for Nonlinear Optics. Hann, R. A., Bloor, D., Eds. *Roy. Soc. Chem.* **1989**, 16.
(50) Pierce, B. M. *Proc. SPIE-Int. Soc. Opt. Eng.* **1991**, *1560*, 148.
(51) Nakano, M.; Yamaguchi, K. *Chem. Phys. Lett.* **1993**, *206*, 285.

Figure 8. Illustration of the optical channels involved for each of the terms (D, N, and T) of the three-term expression for γ.

$|e'\rangle$ ($|n\rangle$ in eq 3):

$$\gamma_{XXXX[\text{model}]} =$$

$$24\frac{\langle g|\mu_X|e\rangle(\langle e|\mu_X|e\rangle - \langle g|\mu_X|g\rangle)(\langle e|\mu_X|e\rangle - \langle g|\mu_X|g\rangle)\langle e|\mu_X|g\rangle}{E_{ge}^3}$$

$$- 24\frac{\langle g|\mu_X|e\rangle\langle e|\mu_X|g\rangle\langle g|\mu_X|e\rangle\langle e|\mu_X|g\rangle}{E_{ge}^3}$$

$$+ 24\sum_{e'}\frac{\langle g|\mu_X|e\rangle\langle e|\mu_X|e'\rangle\langle e'|\mu_X|e\rangle\langle e|\mu_X|g\rangle}{E_{ge}^2 E_{ge'}} \qquad (7)$$

$$\gamma_{XXXX[\text{model}]} = 24\frac{M_{ge}^2\Delta\mu^2}{E_{ge}^3} - 24\frac{M_{ge}^4}{E_{ge}^3} + 24\sum_{e'}\frac{M_{ge}^2 M_{ee'}^2}{E_{ge}^2 E_{ge'}} \qquad (8)$$

term notation: **D**   **N**   **T**

There appears three terms that correspond to the following: (i) The **D** (dipolar) term, as in the case of $\beta_{XXX[\text{model}]}$, is explicitly dependent on $\Delta\mu$, M_{ge}^2, and E_{ge} (it thus provides a positive contribution). (ii) The **N** (negative) term gives net negative contribution and, as for $\alpha_{XXX[\text{model}]}$, only depends on M_{ge} and E_{ge}. Taken together, these first two terms constitute the so-called two-state model for γ where only the ground state and the first excited state are considered to contribute to the description of the hyperpolarizability. (iii) A third term, the **T** ("two-photon") term, which also must be introduced, takes into account the participation of higher excited states $|e'\rangle$ within two-photon-like processes. In practice, for the DAO molecule, we find that three excited states $|e'\rangle$ provide the most significant contributions of this type. In Figure 8, we illustrate some of the states and the optical channels (virtual transitions) involved for each of these terms.
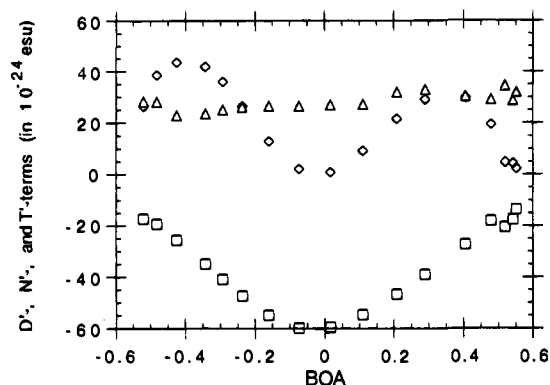
The evolution of these three terms as a function of BOA, as well as $\gamma_{XXXX[\text{SOS}]}$ and $\gamma_{XXXX[\text{model}]}$, is compared in the bottom of Figure 7. It appears that $\gamma_{XXXX[\text{model}]}$ is able to reproduce the overall evolution of the second hyperpolarizability. The **D** term is important since it is responsible for the two positive peaks; if it is neglected or if it vanishes (which is the case in a centrosymmetric system), when starting from the polyene limit and increasing the field, γ would immediately start decreasing and then become negative without showing any positive extremum. The **D** term provides a positive contribution that is maximum in between the polyene and cyanine limits and in between the cyanine and zwitterionic structures; the model is thus able to rationalize the reason why, near the polyene limit, the substitution of a polyene molecule by donor and acceptor groups results in an increase in (positive) γ, as discussed by Garito et al.[49b] The **T** term is always positive and presents a maximum at the cyanine limit; it directly counteracts the

Figure 9. Evolution in DAO of the **D′** (diamonds), **N′** (squares), and **T′** terms (triangles) plotted *vs* BOA.

influence of the **N** term, which also peaks at the cyanine limit. The **T** term thus contributes to making the $\gamma_{xxxx}^{[model]}$ value able to reproduce more accurately the magnitude of γ_{xxxx} at different BOA values.

In the strongly bond alternated structures, the combination of the **D** and **T** terms leads to positive γ values. With decreasing BOA, the **N** term rapidly increases in magnitude, reaching a peak at the cyanine limit where $\Delta\mu$ and therefore the **D** term vanish; globally, around the cyanine limit γ is then negative since the magnitude of the **N** term is larger than that of the **T** term, due to the very large values of $1/E_{ge}$ and M_{ge}, relative to $1/E_{ge'}$ and $M_{ee'}$.

It is also informative to rewrite eq 8 by taking out the common terms:[50,52]

$$\gamma_{model} = 24\frac{M_{ge}^{2}}{E_{ge}^{2}}\left(\frac{\Delta\mu_{ge}^{2}}{E_{ge}} - \frac{M_{ge}^{2}}{E_{ge}} + \sum_{e'}\frac{M_{ee'}^{2}}{E_{ge'}}\right) \quad (9)$$

term notation: **D′**   **N′**   **T′**

The **D′**, **N′**, and **T′** terms from eq 9 have the same dimensionality as α; their evolutions as a function of BOA are plotted in Figure 9. The interesting aspect is that the two-photon term **T′** remains roughly constant over the whole range of bond alternation evolution and is in effect a positive offset. Its relative role is particularly important in the polyene limit and is in fact responsible for the positive γ of polyenes. Figure 9 suggests that the optimization of γ has to focus on the **D** and **N** terms and also points out the inadequacy of the scaling arguments used to link the γ values to the α values;[53] while α simply increases with decreasing magnitudes of bond alternation, γ has a more complex evolution.

Recently, Marder and co-workers[18,54] have reported the solvent dependence of γ for a variety of push−pull molecules. These solvent-dependent results were associated with changes in molecular geometry and did allow a buildup of the γ curve, as reproduced theoretically in our work as a function of BOA. These results provide structural guidelines for the optimization of γ in either a positive or negative sense.

VI. From a Donor−Acceptor Polyene to a Cyanine Molecule

Previous theoretical[50,55−58] and experimental[43,59] studies have shown that cyanines constitute a most interesting class of molecules. In particular, these studies point out the following features: (i) the linear polarizability α of a cyanine is intrinsically higher than that of a polyene or an aromatic compound with an equivalent number of π-electrons; (ii) in contrast to a merocyanine such as DAO, the cyanines do not show a solvent dependence of the polarizability α; and (iii) the molecular geometry of linear cyanine cations has a dramatic effect on the sign and magnitude of γ [γ is negative with a symmetric geometry (BLA = 0), but becomes positive when a certain amount of bond alternation is introduced].

We investigate a symmetric cyanine cation related to DAO, *i.e.*, $[(CH_3)_2N(CH=CH)_4CH=N(CH_3)_2]^+$ using the same theoretical approach as above, and the electric field dependent properties are calculated. This cyanine molecule (Figure 2) possesses C_{2v} symmetry and has roughly zero BLA and BOA. The charge distribution is therefore identical around the two end groups, and the state dipole moments are equal to zero along the long axis of the molecule.

The intrinsic molecular geometry of this cyanine molecule in the absence of an external electric field is similar to that calculated for DAO when an external electric field of approximately 5×10^7 V/cm is applied along the long axis of DAO. However, under the influence of a field of the same order of magnitude, the cyanine acquires a molecular structure that becomes polyene-like (or zwitterionic-like, which arbitrarily depends on the direction of the applied field), where BOA is no longer equal to zero.

In Figure 6, we display the evolutions of the transition energies as a function of BOA for the cyanine molecule, in comparison to that for DAO. The similarities between the two evolutions are clearly apparent. We can thus state that E_{ge} minimizes at the cyanine limit for the given molecule while M_{ge} maximizes at this limit (see top of Figure 7). As for DAO, the evolution of $\Delta\mu$ for the cyanine molecule presents two extrema between the polyene and the cyanine limits and between the cyanine and zwitterionic limits, respectively; at the cyanine limit, $\Delta\mu$ goes through zero (and changes its sign).

When evaluated using the model expressions for α, β, and γ, the electric field dependence of the molecular polarizabilities for the cyanine molecule reproduces the evolution and the magnitude obtained with the SOS expressions, as has been previously observed for DAO. In Figure 10, the evolutions, as a function of BOA, of $\gamma_{xxxx}^{[model]}$, **N** term, **T** term are plotted for both the cyanine molecule and DAO. From that figure, it can be seen that at the cyanine limit, the absolute value of $\gamma_{xxxx}^{[model]}$ is larger in DAO than in the cyanine molecule. In fact, since the **D** term is zero at that limit, only the **N** and **T** terms contribute to $\gamma_{xxxx}^{[model]}$; the magnitude of γ_{xxxx} is then controlled by the balance between these two terms of opposite signs. It turns out that the **N** terms are almost equal in both cases, since M_{ge} and E_{ge} are similar. On the other hand, the **T** term is smaller in DAO than in the cyanine. The **T** terms differ not only in magnitude (108 × 10⁻³⁴ esu for DAO when $F = 5 \times 10^7$ V/cm and 157 × 10⁻³⁴ esu for the cyanine compound) but also in the nature of the contributions; for DAO, three $|e'\rangle$

(52) Meyers, F.; Marder, S. R.; Pierce, B. M.; Brédas, J. L. *Chem. Phys. Lett.*, in press.

(53) Agrawal, G. P.; Cojan, C.; Flytzanis, C. *Phys. Rev. B* **1978**, *17*, 776.

(54) Marder, S. R.; Gorman, C. B.; Meyers, F.; Perry, J. W.; Bourhill, G.; Brédas, J. L.; Pierce, B. M. *Science* **1994**, *265*, 632.

(55) Rustagi, K. C.; Ducuing, J. *Opt. Commun.* **1974**, *10*, 258. Mehendale, S. C.; Rustagi, K. C. *Opt. Commun.* **1979**, *28*, 359.
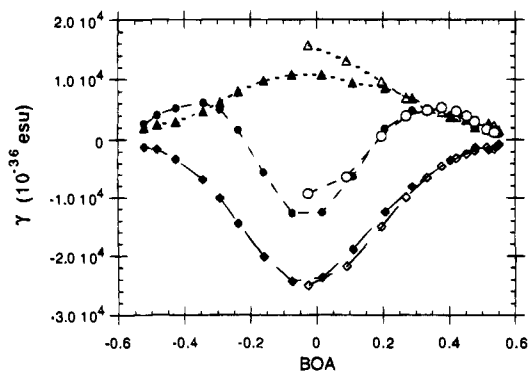
(56) Bodart, V. P.; Delhalle, J.; André, J. M. in ref 5, p 509.

(57) Marder, S. R.; Gorman, C. B.; Cheng, L. T.; Tiemann, B. G. *Proc. SPIE-Int. Soc. Opt. Eng.* **1992**, *1775*, 19.
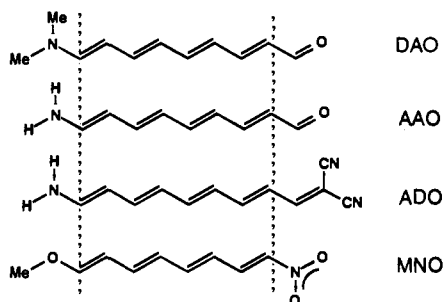
(58) Schulten, K.; Dinur, U.; Honig, B. *J. Chem. Phys.* **1980**, *73*, 3927.

(59) Stevenson, S. H.; Donald, D. S.; Meredith, G. R. in ref 3, p 103.

Figure 10. Evolution versus BOA for the 9-(dimethylamino)nona-2,4,6,8-tetraenal molecule, DAO (full symbols), and the cyanine molecule (open symbols) of $\gamma_{xxxx}^{[model]}$ (circles), N term (diamonds), and T term (triangles).

Figure 11. Sketch of the donor—acceptor polyene molecules investigated in this work: the 9-(dimethylamino)nona-2,4,6,8-tetraenal molecule, DAO; octatetraene end-capped by amino and aldehyde groups, AAO, by amino and dicyanovinyl groups, ADO, and by methoxy and nitro groups, MNO.

states provide significant contributions, whereas for the cyanine molecule, there is a single $|e'\rangle$ state that dominates the T term; interestingly, in the cyanine, the very large $M_{ee'}$ transition dipole is actually of the same order of magnitude as M_{ge}.

From the comparison between DAO and the cyanine molecule, it turns out that the positive maximum of γ is reached at the same BOA value; the absolute magnitude is there, in both cases, about twice as small as in the cyanine limit. In the strongly bond alternated form, both molecules present a positive and relatively small γ_{xxxx} value (Figure 10).

Finally, we stress that the similarities in the description of DAO and the equivalent cyanine compound confirm that the approach of using an external static electric field to tune the molecular structure as a function of the ground-state polarization is reasonable and thus provides a unified model for the characterization of the NLO response in polymethines in general.[54]

VII. Varying the Donor and/or Acceptor Substituents

Three other noncentrosymmetric molecules, whose structures are shown in Figure 11, have also been investigated using the same approach. These molecules all have a polyenic conjugated segment of the same length as in DAO (*i.e.*, octatetraene) but are end-capped by different donor and acceptor substituents: amino and aldehyde groups (AAO); amino and dicyanovinyl groups (ADO); and methoxy and nitro groups (MNO). The external static electric field is applied along the long axis of the molecule, as in the case of DAO.

The evolutions of BLA as a function of F (Figure 12) are qualitatively independent of the types of substituents. We observe the following: (i) When $F = 0$, the BLA value is about the same for all four compounds depicted in Figure 11; it ranges
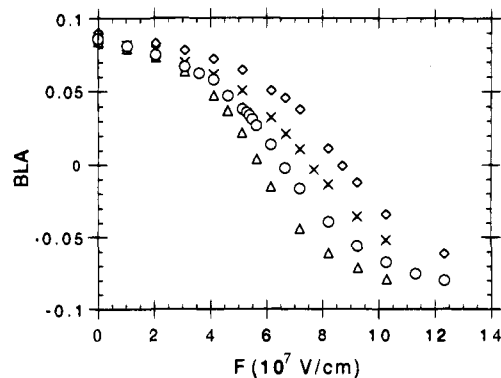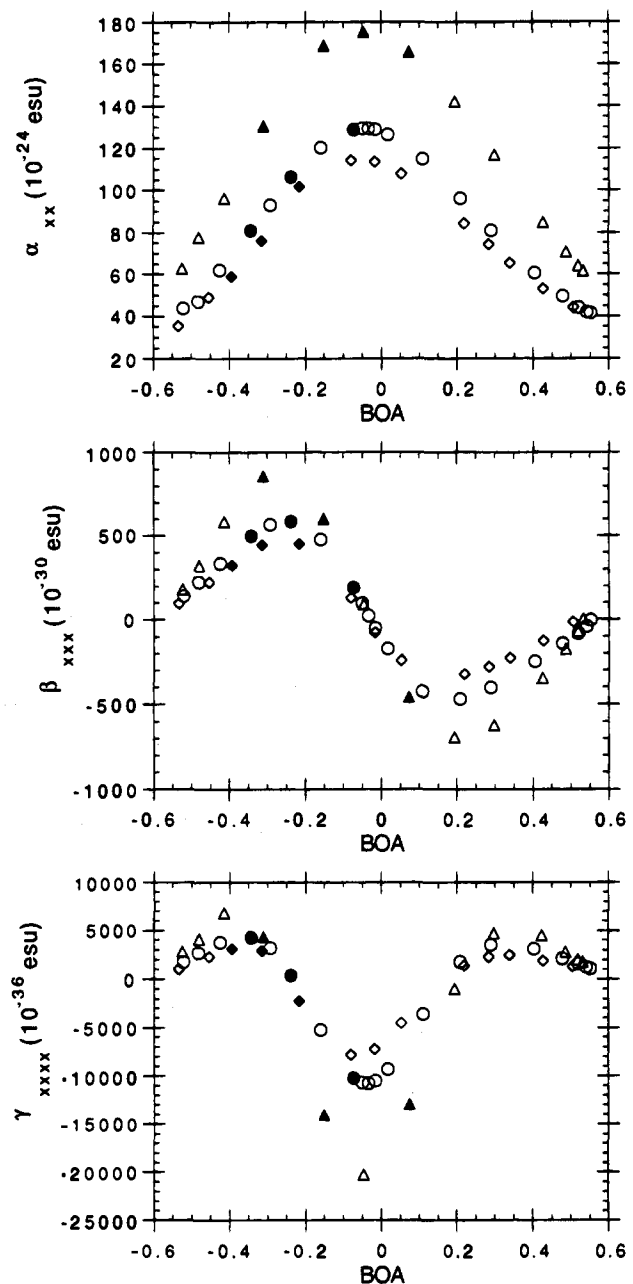

Figure 12. Evolution of the bond length alternation, BLA (in Å), as a function of applied external field F for the substituted polyenes: DAO (circles); AAO (crosses); ADO (triangles); and MNO (diamonds).

from 0.090 Å in the MNO compound to 0.084 Å in ADO. (ii) The external field required to distort the molecular geometry to a given BLA is inversely proportional to the strength of the donor/acceptor pair. For example, to reach the point where BLA is zero, an external field (denoted F_0) of 8.7×10^7 V/cm must be applied along MNO, the compound with the weakest donor/acceptor pair. This field is reduced to 7.7×10^7 V/cm for AAO, and 6.6×10^7 V/cm for DAO. The stronger donor/acceptor pair in ADO leads to $F_0 = 5.8 \times 10^7$ V/cm. Accordingly, for a given external field value, the stronger the donor—acceptor pair, the more the structure is driven away from the polyene limit. For example, for a field of 6.2×10^7 V/cm, the BLA values are -0.015 Å in ADO (*i.e.*, the bond alternation pattern in this compound is already slightly reversed), $+0.014$ Å in DAO, $+0.033$ Å in AAO, and $+0.051$ Å in MNO which presents the weaker donor/acceptor pair.

As defined in Section III, the magnitude of the internal electric field F_i, associated with a pair of substituents, is a manifestation of their donor/acceptor strength (the larger the donor/acceptor strength, the larger the effective internal field value F_i). We calculated the F_i values to be equal to 6.0×10^7, 6.5×10^7, and 7.5×10^7 V/cm for MNO, AAO, and ADO, respectively, to be compared to 7.0×10^7 V/cm for DAO. Thus, the more intense the internal field, the lower the magnitude of the applied external field needed to significantly perturb the molecular structure.

The electric field dependences of the NLO properties for these donor/acceptor substituted octatetraenes, plotted as a function of BOA, are consistent with those for DAO (Figure 13). It must be stressed that the extrema in the α, β, and γ curves occur at *identical BOA values* for the various molecules. However, the magnitudes at the peaks do depend on the exact nature of the donor and acceptor substituents. Among the compounds investigated here, the ADO molecule always presents the largest peak values (however, note that it is two atoms longer than the other molecules), while the smallest values are calculated for MNO.

The evolutions of the NLO properties for the substituted octatetraenes can also be examined as a function of F. In this manner, the analysis becomes similar to the solvent-dependent hyperpolarizability measurements that are feasible experimentally.[17,18] Indeed, in a first approximation, an external electric field acts on a molecule in the same way as the reaction field caused by the surrounding solvent.[60] In Table 2, we compare for the MNO, DAO, and ADO compounds the evolutions of β_{xxx} and γ_{xxxx}, within a range of electric fields of $F = 3$ to 5×10^7 V/cm. In the following discussion, the key comparisons

---

(60) Liptay, W. *Angew. Chem., Int. Ed. Engl.* **1969**, *8*, 177.

10712 *J. Am. Chem. Soc., Vol. 116, No. 23, 1994*

Meyers et al.

Figure 13. Evolutions vs BOA of (top) α_{xx}[SOS] in 10^{-24} esu, (middle) β_{xxx}[SOS] in 10^{-30} esu, and (bottom) γ_{xxxx}[SOS] in 10^{-36} esu for the substituted polyenes: DAO (circles); ADO (triangles); and MNO (diamonds). The filled symbols correspond to the data also reported in Table 2 (see text).

Table 2. Field Dependence (from $F = 3$ to 5×10^7 V/cm) of the First (β_{xxx}, Top Entries, in 10^{-30} esu) and Second (γ_{xxxx}, Bottom Entries, in 10^{-36} esu) Hyperpolarizabilities for the Substituted Octatetraene Molecules MNO, DAO, and ADO[a]

		F (10^7 V/cm)		
		3	4	5
MNO	β_{xxx}	323	443	452
	γ_{xxxx}	3076	2916	−2196
DAO	β_{xxx}	497	587	191
	γ_{xxxx}	4587	339	−10217
ADO	β_{xxx}	858	603	−458
	γ_{xxxx}	4346	−14039	−12921

[a] The corresponding data, plotted versus BOA, are outlined with the solid symbols in Figure 13.

are not between the absolute magnitudes of the hyperpolarizabilities but rather their trends. When F goes from 3 to 5 ×
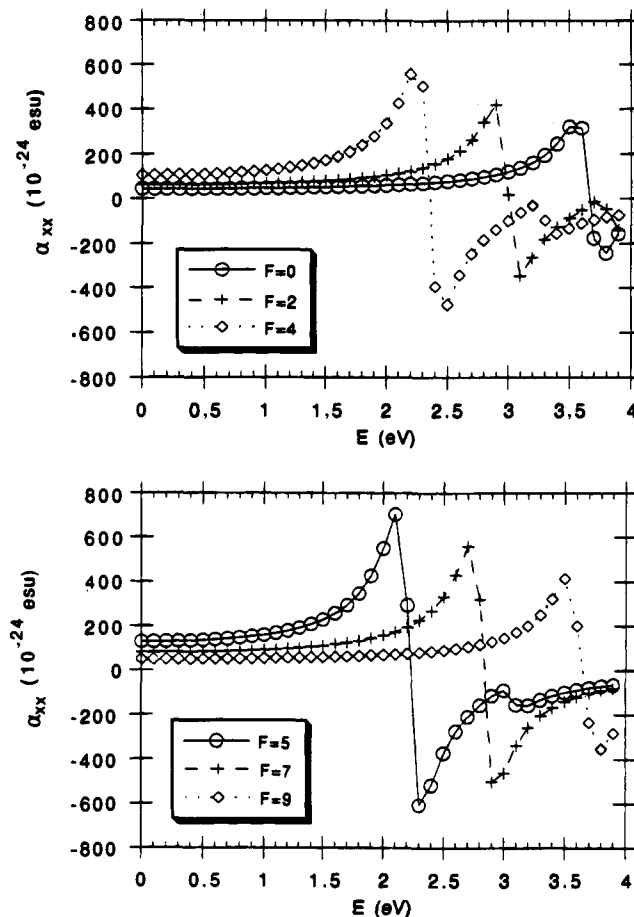
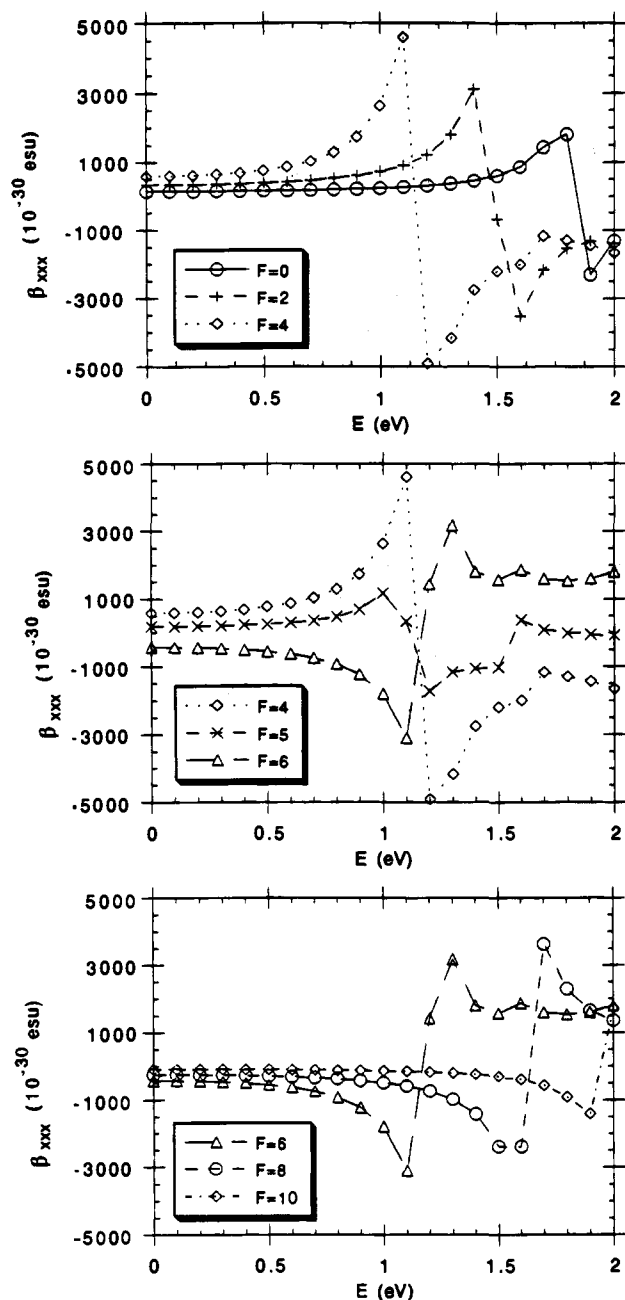**Figure 14.** Evolution of Re[$\alpha_{xx}(-\omega;\omega)$] in DAO as a function of fundamental energy, E ($=\hbar\omega$), for different values of the external electric field F expressed in units of 10^7 V/cm.

10^7 V/cm, we observe that β_{xxx} steadily increases for MNO, that it peaks around $F = 4 \times 10^7$ V/cm for DAO, and that it changes sign between $F = 4$ and 5×10^7 V/cm for ADO. On the other hand, γ_{xxxx} decreases and changes sign between $F = 4$ and 5×10^7 V/cm for MNO and DAO and between $F = 3$ and 4×10^7 V/cm for ADO. For a more convenient comparison, the corresponding data are indicated by filled symbols in Figure 13. It is important to emphasize that the changes in the evolutions of β_{xxx} and γ_{xxxx} when increasing the external field F are qualitatively comparable to those observed experimentally when increasing the polarity of the solvent.[54] Both analyses, based on experimental and theoretical results, have contributed to determine the derivative relationships existing between α, β, and γ.[54]

VIII. Dynamic Properties

The computation of the NLO properties using the SOS approach[29] also allows for an easy simulation of dynamic (frequency-dependent) processes: at first order, $\alpha(\omega;\omega)$; at second order, for instance second-harmonic-generation $\beta(-2\omega;\omega,\omega)$; and at third-order, for instance third-harmonic-generation $\gamma(-3\omega;\omega,\omega,\omega)$. The frequency-dispersion analysis has been performed on DAO and is reported in Figures 14−16 for different values of applied external electric field F. Our goal here is to ascertain that the evolutions we have calculated at the static limit also hold when explicitly considering the optical frequencies used in actual experiments.

The lowest resonances at E_{ge}, $E_{ge}/2$, and $E_{ge}/3$ in the cases of $\alpha(-\omega;\omega)$, $\beta(-2\omega;\omega,\omega)$, and $\gamma(-3\omega;\omega,\omega,\omega)$, respectively, are clearly observed and followed the evolution of the first transition
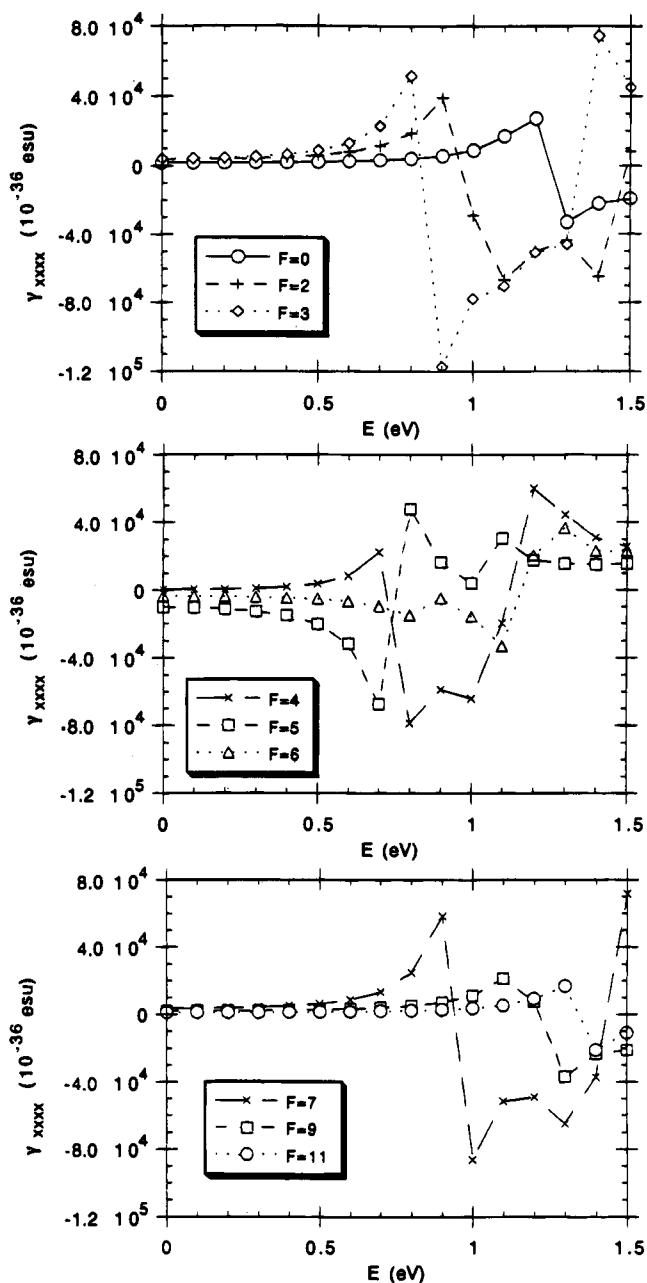
Figure 15. Evolution of $Re[\beta_{xxx}(-2\omega;\omega,\omega)]$ in DAO as a function of fundamental energy, E ($=\hbar\omega$), for different values of the external electric field F expressed in units of 10^7 V/cm.

Figure 16. Evolution of $Re[\gamma_{xxxx}(-3\omega;\omega,\omega,\omega)]$ in DAO as a function of fundamental energy, E ($=\hbar\omega$), for different values of the external electric field F expressed in units of 10^7 V/cm.

energy as a function of F, as reported above. Furthermore, it is also seen that the larger the static polarizability, the larger the real part of the polarizability before the lowest resonance. As a result, all the conclusions drawn for the static responses of DAO remain valid when dynamic processes are considered.

IX. Synopsis

We have presented a detailed theoretical analysis of the influence of an external static electric field applied along a donor—acceptor polyene. Our calculations have addressed the evolutions of the following: molecular and electronic structures, charge distributions and dipole moments, electronic transitions, and first-, second-, and third-order polarizabilities. The latter have been evaluated through the Sum-Over-States formulation at the correlated level as well as by means of more simple two-state and three-term models.

Our results emphasize the essential relationship between

molecular structure and NLO properties.[36] From our results, we can draw the following conclusions:

(i) The molecular geometry of a polyenic segment can be completely tuned from a polyene-like (bond alternated) structure, through the cyanine limit (non-alternated), to the fully reversed alternated structure or zwitterionic form, as a function of an external static electric field of increasing strength, applied along the molecule. The field is applied in such a way as to favor the charge transfer from the donor to the acceptor end. As a consequence, the dipole moment increases along with the structural changes.

(ii) As it is strongly related to the molecular geometry, the electronic structure is also affected by the field. The evolution of the lowest excited-state energy as a function of the applied field first displays a red shift followed by a blue shift. The red shift (associated to positive solvatochromism, the ground state being less polar than the excited state) takes place when the molecular structure evolves from the neutral polyene structure

to the cyanine limit, while the blue shift (associated to negative solvatochromism, the ground state becoming more polar than the excited state) occurs with the evolution from the cyanine structure to the fully reversed zwitterionic limit.

(iii) The external field-dependent curves for the molecular polarizabilities α, β, and γ are fully correlated with the molecular structure and show the following:

α is maximum at the cyanine limit.

β first increases, peaks in a positive sense for an intermediate polyene/cyanine structure, decreases, passes through zero at the cyanine limit, becomes negative, and peaks in a negative sense; it then decreases again to become smaller in the zwitterionic limit.

γ presents a more complex evolution; it first increases, peaks positively, decreases, is zero when β peaks, becomes negative, and peaks in a negative sense at the cyanine limit where β is zero. With respect to the cyanine limit, γ presents a symmetric evolution. We note that the shapes of the β and γ evolutions versus BOA are first- and second-derivative-like with respect to the α evolution. These derivative relationships are discussed in detail elsewhere.[54]

(iv) It is remarkable that the α, β, and γ curves present maxima for bond alternations that are identical for the various donor–acceptor polyenes investigated here. This confirms that the bond order alternation or bond length alternation in the molecular structure is an essential parameter determining the NLO response of conjugated organic molecules. The absolute values at the maxima depend on the nature of the donor/acceptor pair.

(v) When analyzing the dynamic responses, such as second- or third-harmonic generation, we obtain trends that indicate that the largest polarizabilities at near-resonance are found for the molecular structures displaying the largest off-resonance values.

In summary, we believe that the calculations performed here are useful in providing a detailed interpretation of the molecular polarizabilities and in understanding their solvent dependence. They can be directly exploited to optimize organic materials for NLO applications.